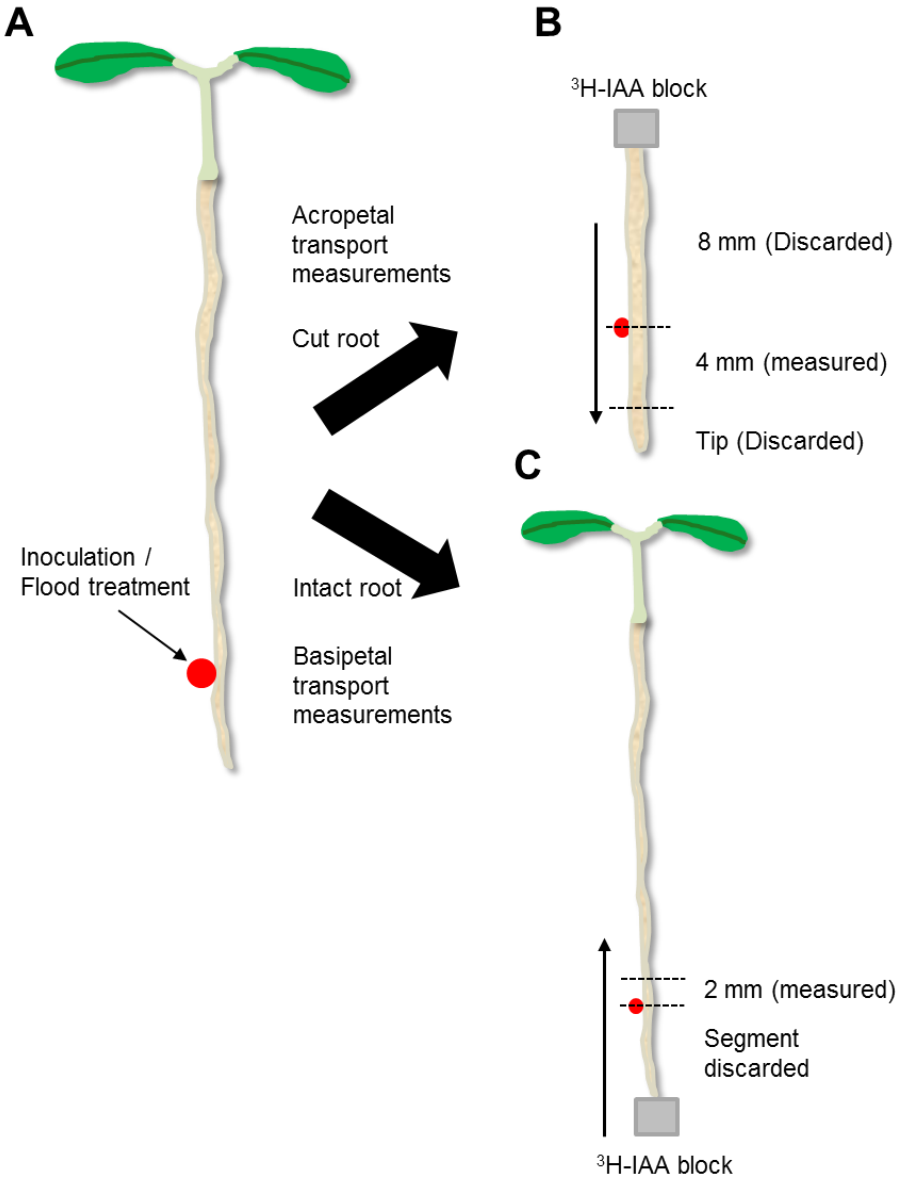
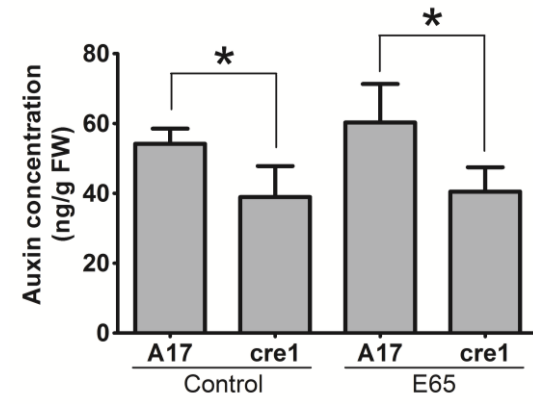


Supplemental Fig. 1. Nodulation efficiency on WT and *cre1* mutant roots spot-inoculated with *Sinorhizobium meloti* strains Rm1021 and E65. Nodules were quantified two weeks post-inoculation. A two-way ANOVA with a Tukey-Kramer multiple comparison post-test was used for statistical analysis ( $p < 0.05$ ,  $n = 20$ ). Different lowercase letters indicate significant differences in nodule numbers per plant. Graphs show mean and SD.



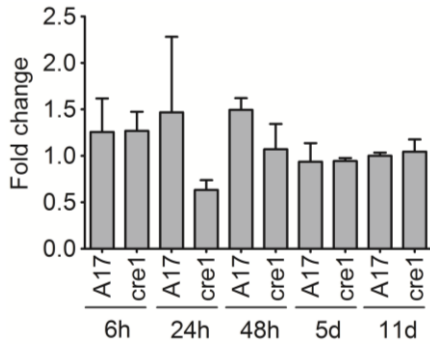
Supplemental Fig. 2. Cartoon showing auxin transport measurements performed in this study. (A) An intact seedling is treated with rhizobia and/or auxin transport inhibitors by spot inoculation or flood treatment. The inoculation site at the zone of emerging root hairs is marked on the plate for reference and roots incubated for a specified time. For acropetal transport measurements (B), the root is excised 8 mm above the inoculation spot, or an equivalent spot in a flood-treated root. The cut root is incubated with a  $^3\text{H}$ -IAA-containing agar block touching the cut end. The 8 mm segment directly touching the block is discarded and radioactivity in the segment below the inoculation spot is measured. For basipetal auxin transport measurements (C), an intact seedling is incubated with a  $^3\text{H}$ -IAA-containing agar block touching the root tip. The segment directly touching the block (~ 6 mm, depending on root growth) is discarded and radioactivity of a 2 mm segment above the inoculation spot is measured. These assays have been developed in *M. truncatula* (Wasson et al., 2006; Plet et al., 2011), based on similar protocols used in *Arabidopsis* (Lewis and Muday, 2009) and are designed to assess the capacity for polar auxin transport using radiolabelled auxin as a tracer. The amount of radiolabelled auxin that is detected in excised root segments reflects the amount of endogenous auxin (IAA) transported into that root segment. We chose to analyse root segment below and above the inoculation site, respectively, for acro- and basipetal auxin transport measurements to determine how the treatment at the local inoculation site alters the transport of auxin beyond that site. Thus, reduced acropetal auxin transport into the segment below the inoculation site indicates that less auxin is exported into that segment as a result of the local infection by rhizobia. We reported all auxin transport measurements relative to the control roots as we were interested in relative changes of auxin transport in control and treated roots. Absolute auxin transport measurements varied between experiments with every batch of radiolabelled auxin used and were therefore difficult to combine for several independent experiments. [Lewis, D.R. and Muday, G.K. (2009) Measurement of auxin transport in *Arabidopsis thaliana*. *Nature Protocols* 4: 437-451].



Supplemental Fig. 3. Combined auxin concentrations (sum of IAA, IBA and IAA-Ala) in WT (A17) and *cre1* mutant roots mock-treated or inoculated with E65 rhizobia. A Student's *t*-test was used for statistical analyses ( $p < 0.05$ ,  $n = 4-5$ ). Asterisks indicate significant differences in total root auxin concentrations between WT and *cre1* mutants.

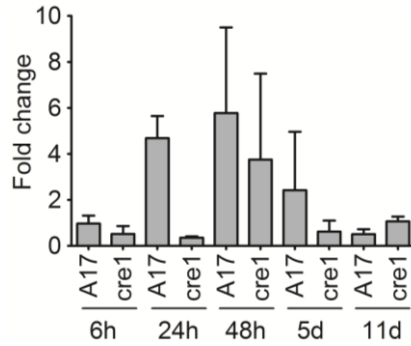
**A**

***PIN1***



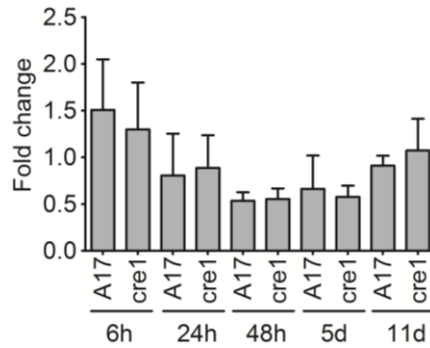
**B**

***PIN2***



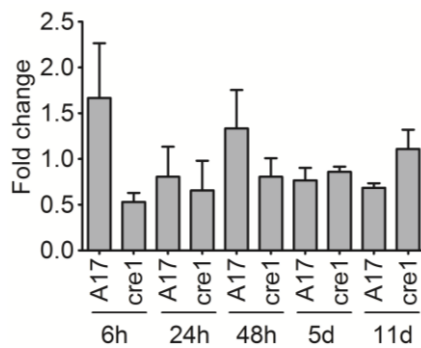
**C**

***PIN3***



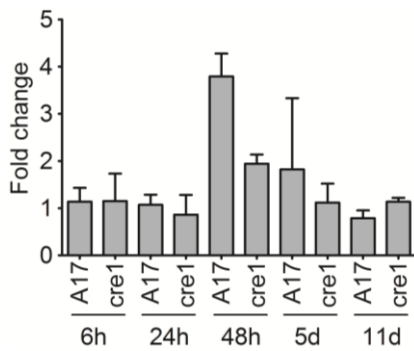
**D**

***PIN4***



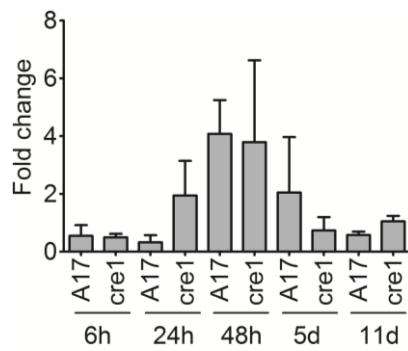
**E**

***PIN6***



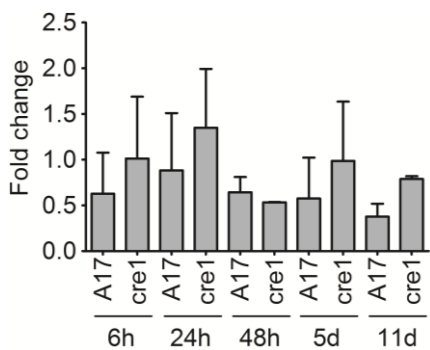
**F**

***PIN7***



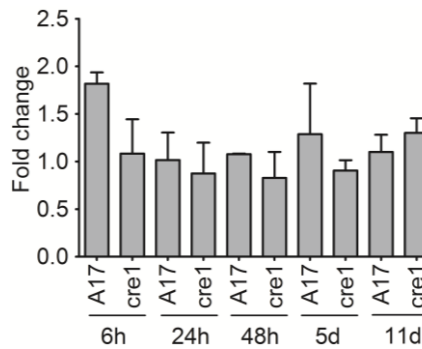
**G**

***PIN9***

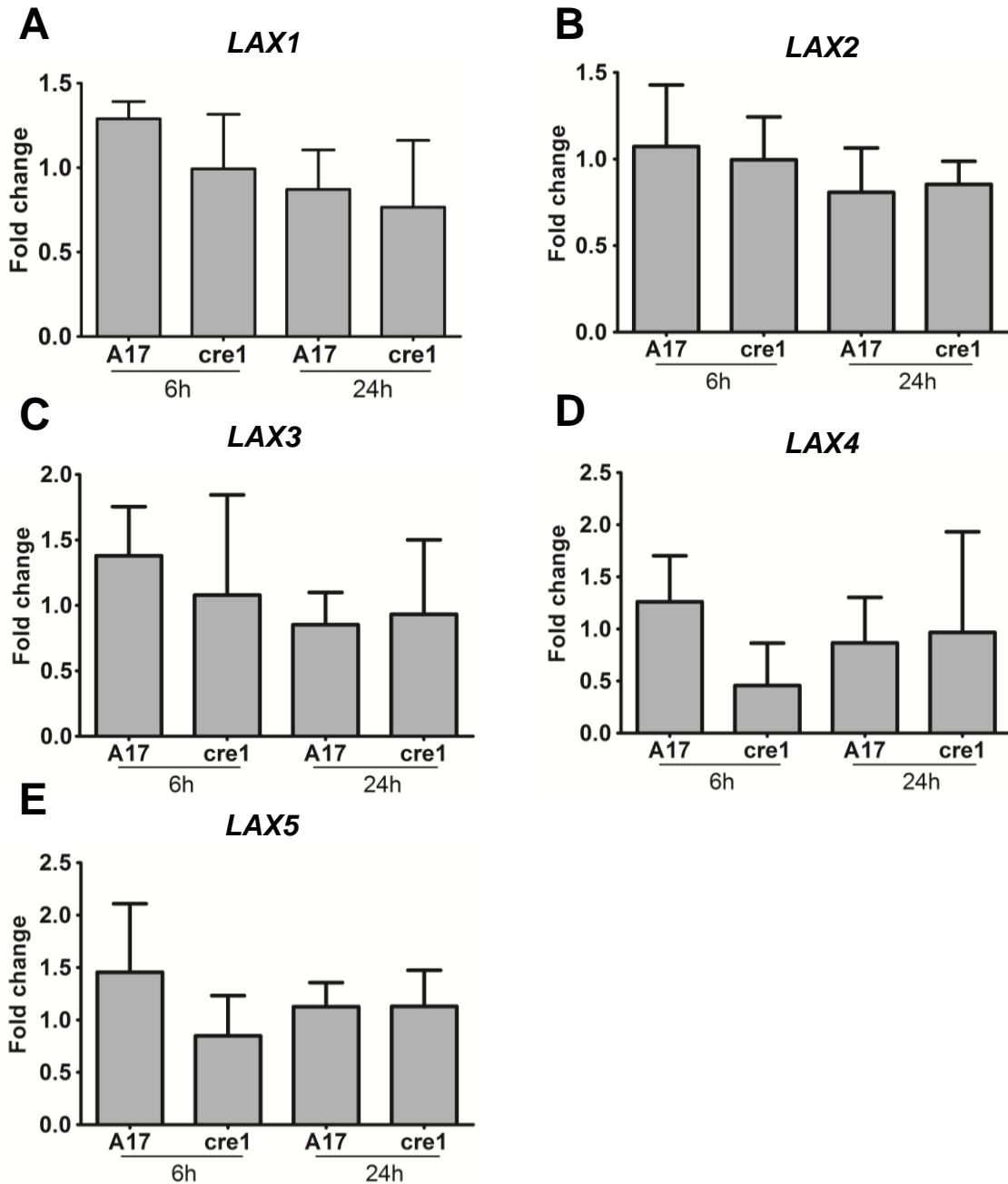


**H**

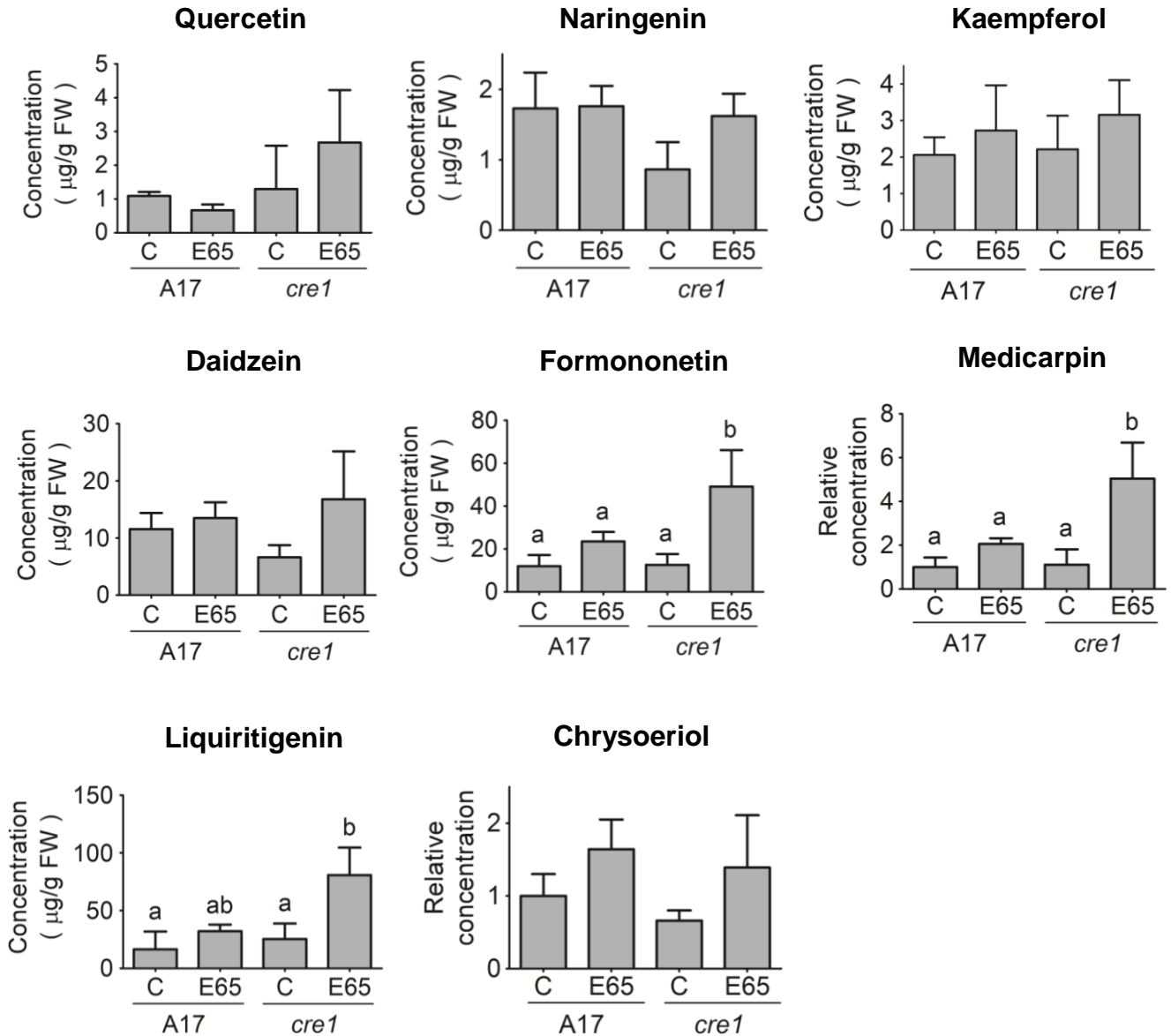
***PIN10***



Supplemental Fig. 4. Quantitative RT-PCR of *PIN* genes. Transcript abundance was quantified in root segments inoculated for 6, 24, 48 h, 5 and 11 d with E65 relatively to mock-treated roots. Expression was normalised to the *GAPDh* reference gene. IAA exporter-encoding genes *PIN1* (A), *PIN2* (B), *PIN3* (C), *PIN4* (D), *PIN6* (E), *PIN7* (F), *PIN9* (G) and *PIN10* (H) were analysed. *PIN5* and *PIN8* mRNAs were not detected in *M. truncatula* roots (Schnabel and Frugoli, 2004). A two-way ANOVA with a Tukey-Kramer multiple comparison post-test was used for statistical analyses ( $p < 0.05$ ,  $n = 3$ ). No significant differences were found between any of the treatments. Three biological replicates consisting of at least 50 individual root segments were analysed. Graphs show mean and SD.

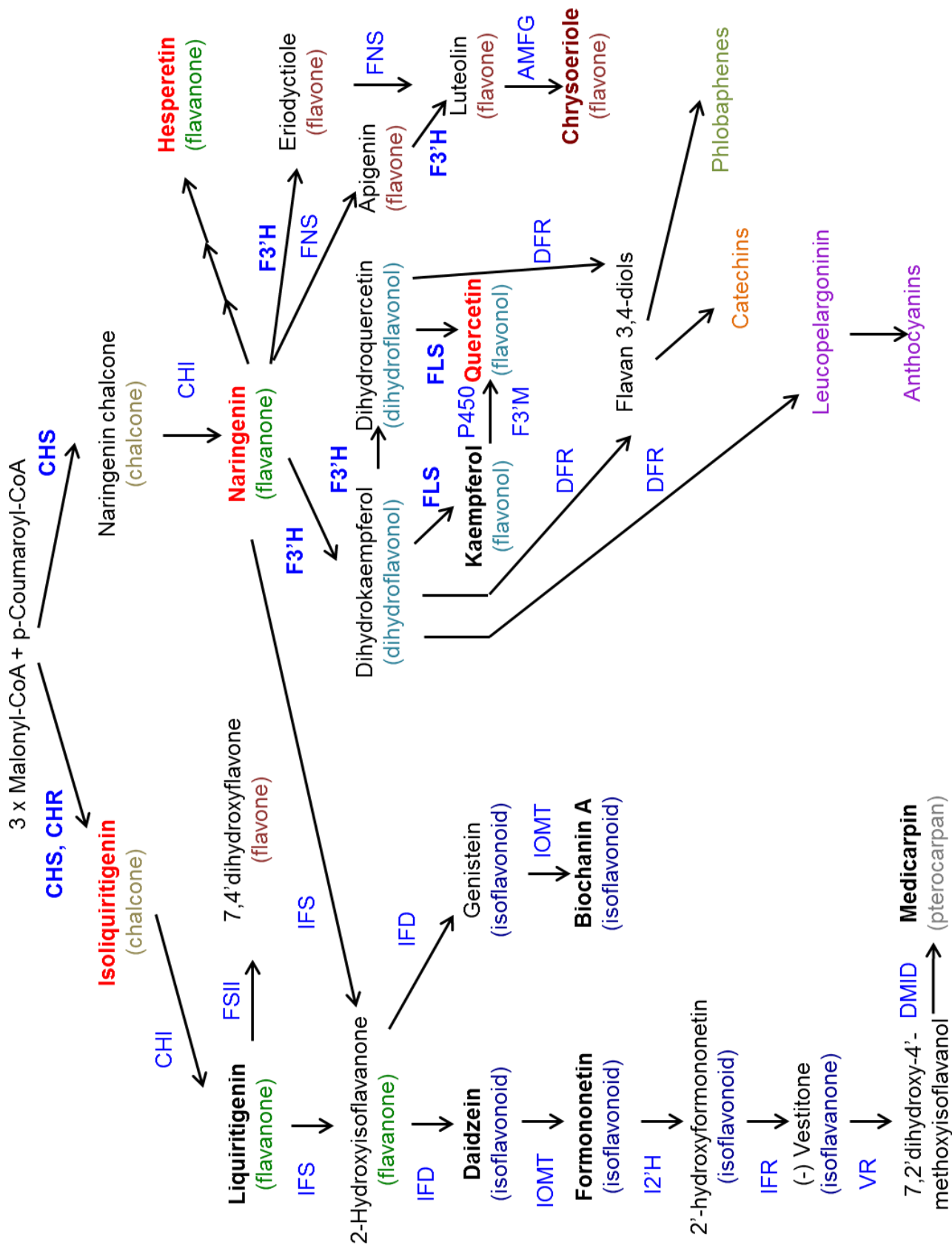


Supplemental Fig. 5. Quantitative RT-PCR of *LAX* genes. Transcript abundance was quantified in root segments inoculated for 6 and 24 h with E65 relatively to mock-treated roots. Expression was normalised to the *GAPDh* reference gene. IAA importer-encoding genes *LAX1* (A), *LAX2* (B), *LAX3* (C), *LAX4* (D), and *LAX5* (E) were analysed. A two-way ANOVA with a Tukey-Kramer multiple comparison post-test was used for statistical analyses ( $p < 0.05$ ,  $n = 3$ ). No significant differences were found between any of the treatments. Three biological replicates consisting of at least 50 individual root segments were analysed. Graphs show mean and SD.

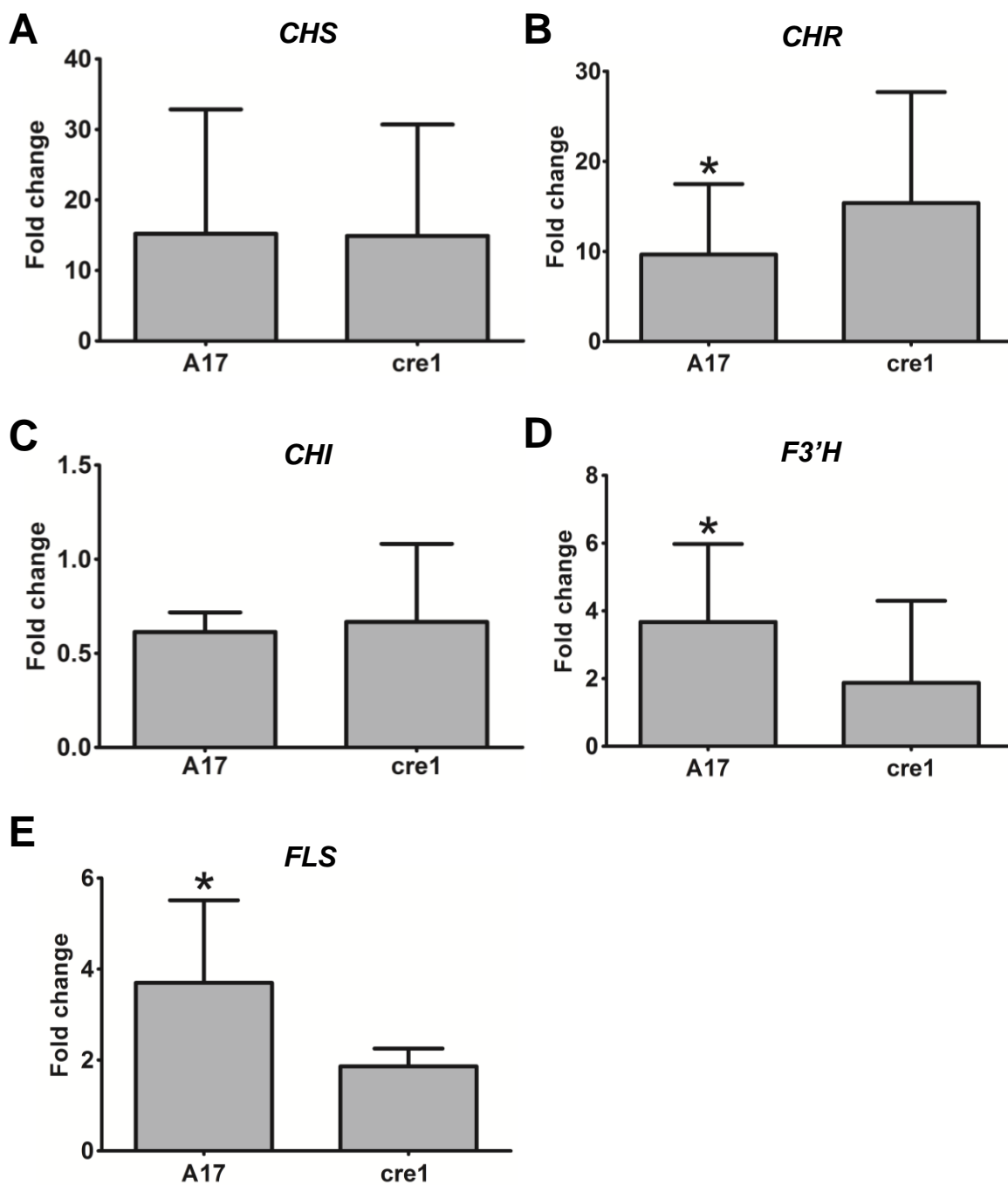


Supplemental Fig. 6. Concentrations of total flavonoid aglycones following acid hydrolysis of flavonoid glycosides in WT and *cre1* roots. The flavonoids quercetin, naringenin, kaempferol, daidzein, formononetin, medicarpin, liquiritigenin and chrysoeriol were analysed in root segments 24 h after mock- or E65 inoculation. A two-way ANOVA with a Tukey-Kramer multiple comparison post-test was used for statistical analyses ( $p < 0.05$ ,  $n = 3$ ). Different lowercase letters indicate significant changes in flavonoid concentrations measured. A total of 15 root segments were harvested for each biological replicate. Graphs show mean and SD.

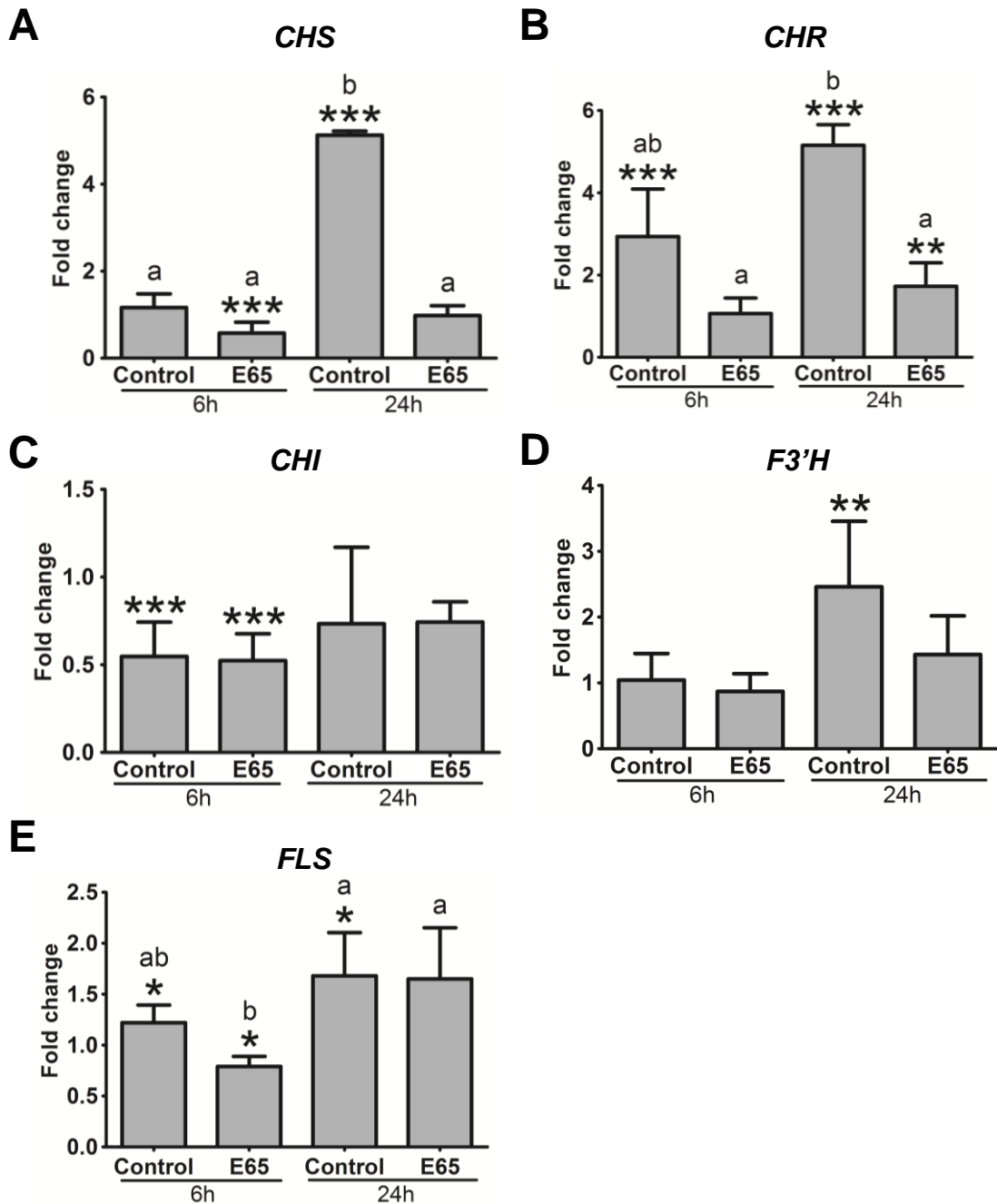




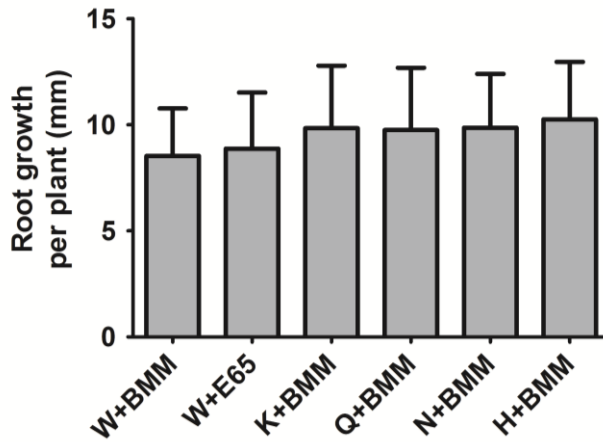
Supplemental Fig. 7. Schematic overview of the flavonoid biosynthesis pathway in *Medicago truncatula*. Aglycones that were detected in the roots are shown in bold. Flavonoids shown in bold red showed differences in induction after inoculation between genotypes (isoliquiritigenin, naringenin, hesperetin and quercetin). Different subclasses of flavonoids are indicated in different colours. Note that we could detect genistein/apigenin but could not differentiate between them because of the identical MW and elution time. Enzymes are shown in blue and are abbreviated as follows: AMFG, S-adenosylmethionine:flavonoid 7-O-glucosyltransferase; CHI, chalcone isomerase; CHR, chalcone reductase; CHS, chalcone synthase; DFR, dihydroflavonol 4-reductase; DMID, 7,2'-dihydroxy-4'-methoxy-isoflavonol dehydratase; F3'H, flavonoid-3'-hydroxylase; F3'M, flavonoid 3'-monooxygenase; FLS, flavonol synthase; FNS, flavone synthase; FSII, Flavone synthase II; I2'H, isoflavone-2'-hydroxylase; IFD, 2-hydroxyisoflavanone dehydratase; IFR, isoflavone reductase; IFS, 2-hydroxyisoflavanone synthase; IOMT, isoflavanone-O-methyltransferase; P450, cytochrome P450; VR, vestitone reductase. Genes encoding enzymes in bold were induced by E65/cytokinin treatment.



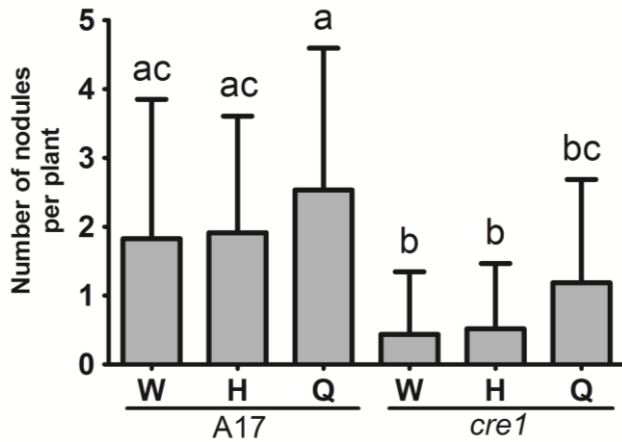
Supplemental Fig. 8. Quantitative RT-PCR showing relative transcript abundance of flavonoid-related genes in roots treated with cytokinin (Benzylaminopurine, BAP). Transcript abundance of flavonoid-related genes in WT (A17) and the *cre1* mutant roots treated with  $10^{-7}$  M BAP for 30 min, relatively to mock-treated roots. Expression was normalised to the *RIBOSOMAL BINDING PROTEIN1* (*RBP1*) reference gene (Plet et al., 2011). (A) *CHALCONE SYNTHASE* (*CHS*), (B) *CHALCONE REDUCTASE* (*CHR*), (C) *CHALCONE ISOMERASE* (*CHI*), (D) *FLAVONOID 3'-HYDROXYLASE* (*F3'H*) and (E) *FLAVONOL SYNTHASE* (*FLS*) genes were analysed. A Student's *t*-test was used for statistical analyses ( $p < 0.05$ ,  $n = 3$ ). Asterisks indicate significant inductions by BAP compared to the mock-treatment in WT. Graphs show mean and SD.



Supplemental Fig. 9. Quantitative RT-PCR showing transcript abundance of flavonoid-related genes in root segments. Transcript abundance of flavonoid-related genes in mock-inoculated (control) and inoculated (E65) roots for 6 and 24 h in *cre1* mutants relatively to WT (A17). Expression was normalised to the *GAPDH* reference gene. (A) *CHALCONE SYNTHASE* (*CHS*), (B) *CHALCONE REDUCTASE* (*CHR*), (C) *CHALCONE ISOMERASE* (*CHI*), (D) *FLAVONOID 3'-HYDROXYLASE* (*F3'H*) and (E) *FLAVONOL SYNTHASE* (*FLS*) genes were analysed. A Student's *t*-test was used for statistical analyses between *cre1* mutants and WT (fold change) ( $p < 0.05$ ,  $n = 3$ ). Asterisks indicate significant differences in induction / repression in *cre1* mutants relative to WT. A two-way ANOVA with a Tukey-Kramer multiple comparison post-test was used for statistical analyses between control and E65 treatments ( $p < 0.05$ ,  $n = 3$ ). Different lowercase letters indicate significant differences in induction / repression between control and E65 treatments. Graphs show mean and SD.



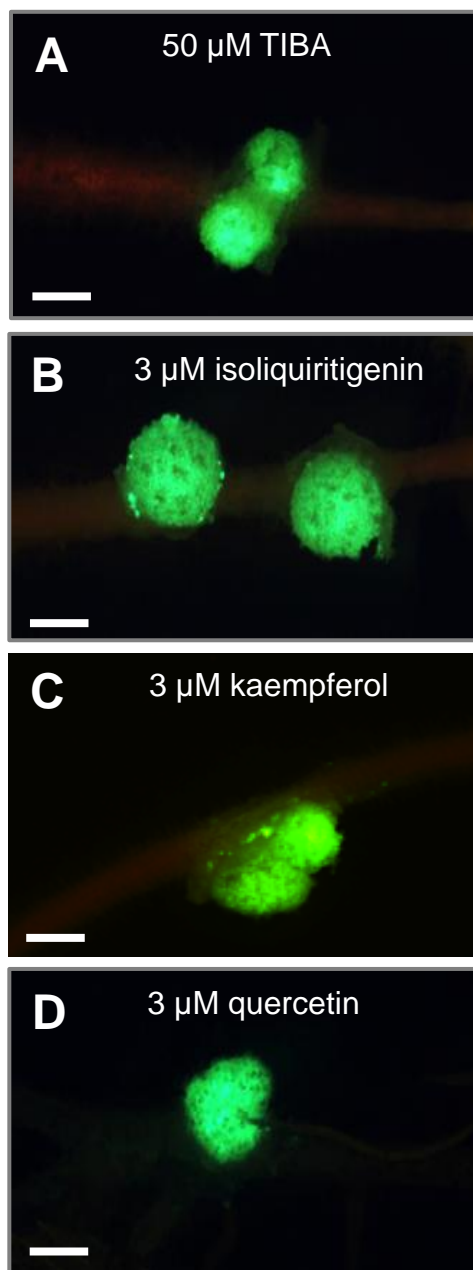
Supplemental Fig. 10. Root growth on *Medicago truncatula* WT plants with or without flavonoids and E65. A Tukey-Kramer multiple comparison test was used for statistical comparison between treatments ( $p < 0.05$ ,  $n = 15$ ). Abbreviations: W, water; K, 3  $\mu\text{M}$  kaempferol; Q, 3  $\mu\text{M}$  quercetin; N, 3  $\mu\text{M}$  naringenin; H, 3  $\mu\text{M}$  hesperetin.

**A****B**

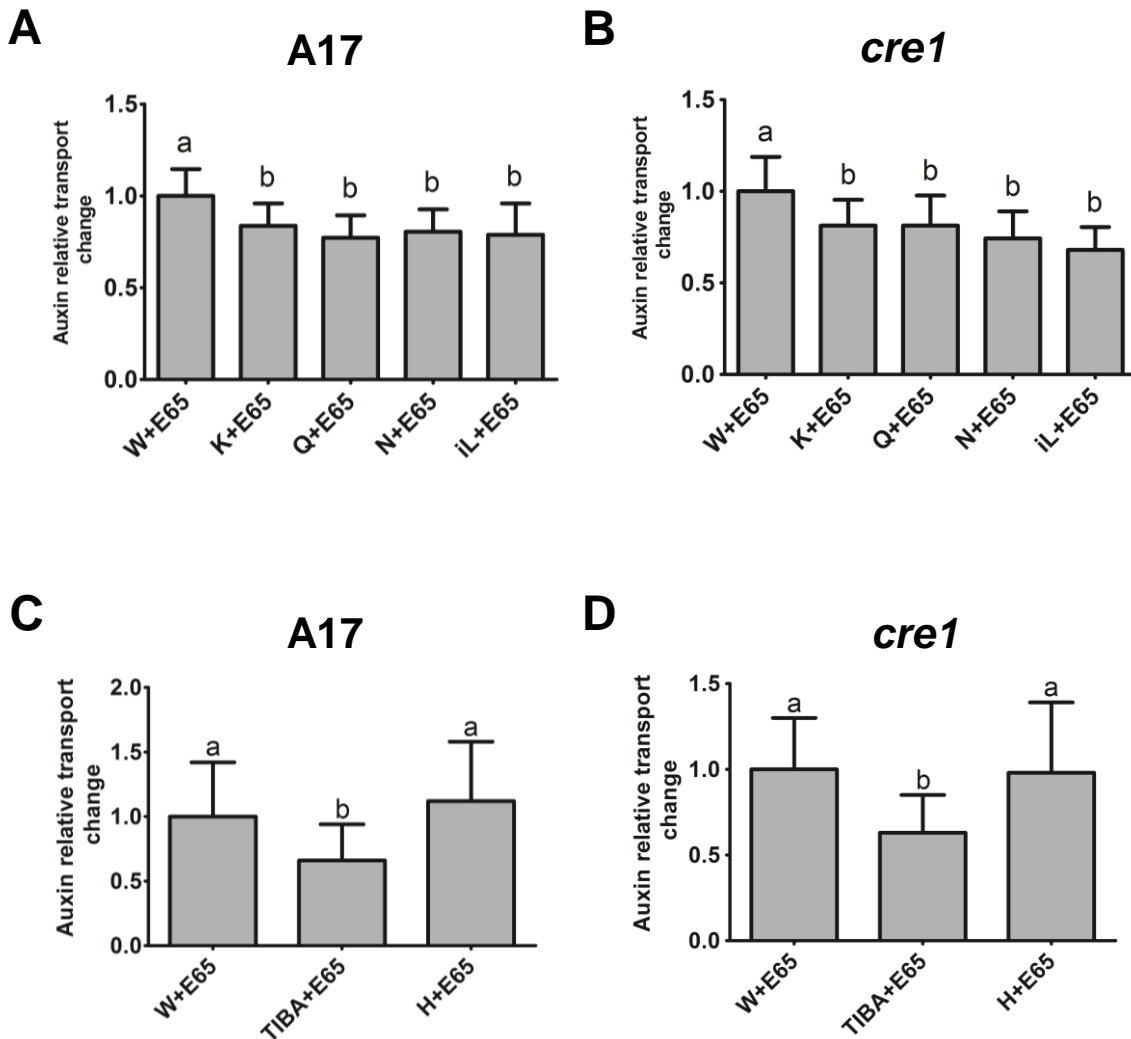
A17			<i>cre1</i>		
W	H	Q	W	H	Q
67	79	77	24	31	58

\*\*

Supplemental Fig. 11. Nodulation on WT and *cre1* mutant roots treated with or without quercetin or hesperetin, in the presence of E65. (A) Nodule formation on A17 and *cre1* mutant roots treated with or without quercetin or hesperetin, in the presence of E65. A two-way ANOVA with a Tukey-Kramer multiple comparison post-test was used for statistical comparison between treatments ( $p < 0.05$ ,  $n = 35$ ). (B) Percentage of plants forming nodules on WT (A17) and *cre1* mutant roots treated with or without quercetin or hesperetin, in the presence of E65. A two-sample Student's *t*-test was used for statistical comparison between treatments (\*\*  $p < 0.01$ ,  $n = 35$ ). Abbreviations: W, water; H, 3  $\mu$ M hesperetin; Q, 3  $\mu$ M quercetin.

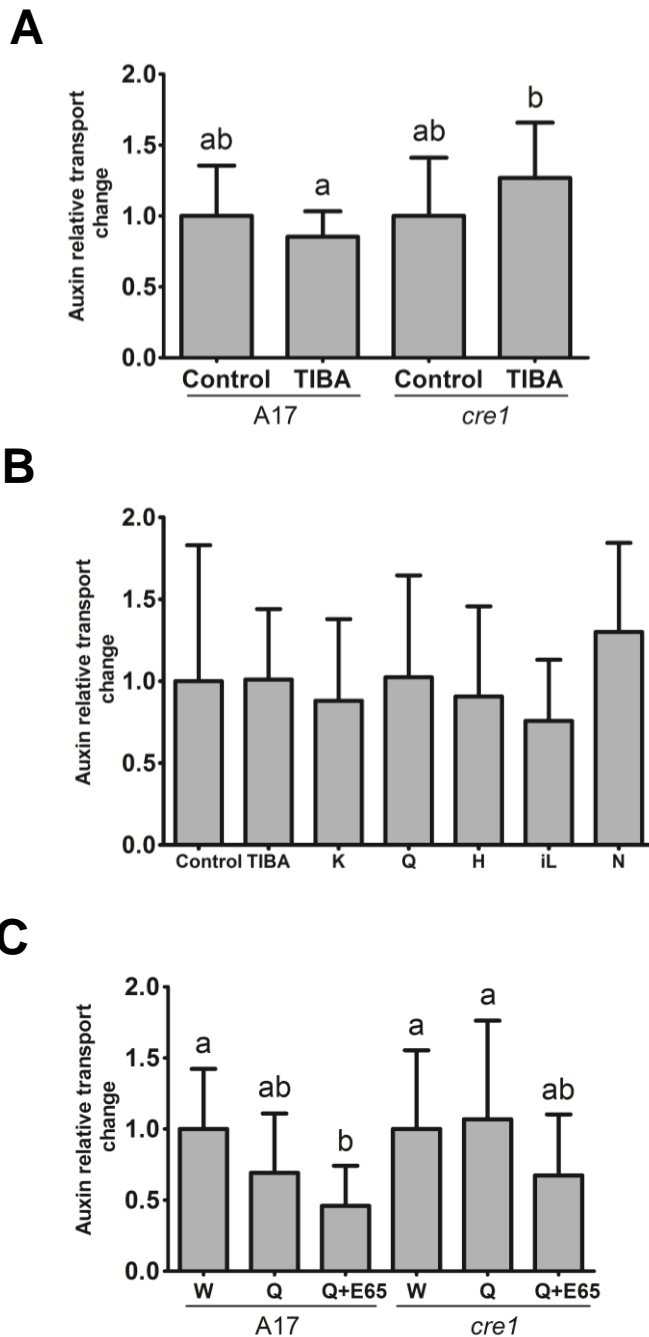


Supplemental Fig. 12. Nodules formed on *cre1* mutant roots with addition of auxin transport inhibitors are infected by rhizobia. Roots were co-flood-inoculated with each auxin transport inhibitor and a *gfp*-expressing Sm1021 E65 strain. Nodules were photographed at 3 weeks p.i.. (A) TIBA-, (B) isoliquiritigenin-, (C) kaempferol- and (D) quercetin-rescued nodules. Images were taken under GFP excitation (max. excitation 470 nm; 515 nm longpass filter). More than 20 nodule-forming roots were observed with fluorescence for each treatment. Scale bars represent 1 mm.

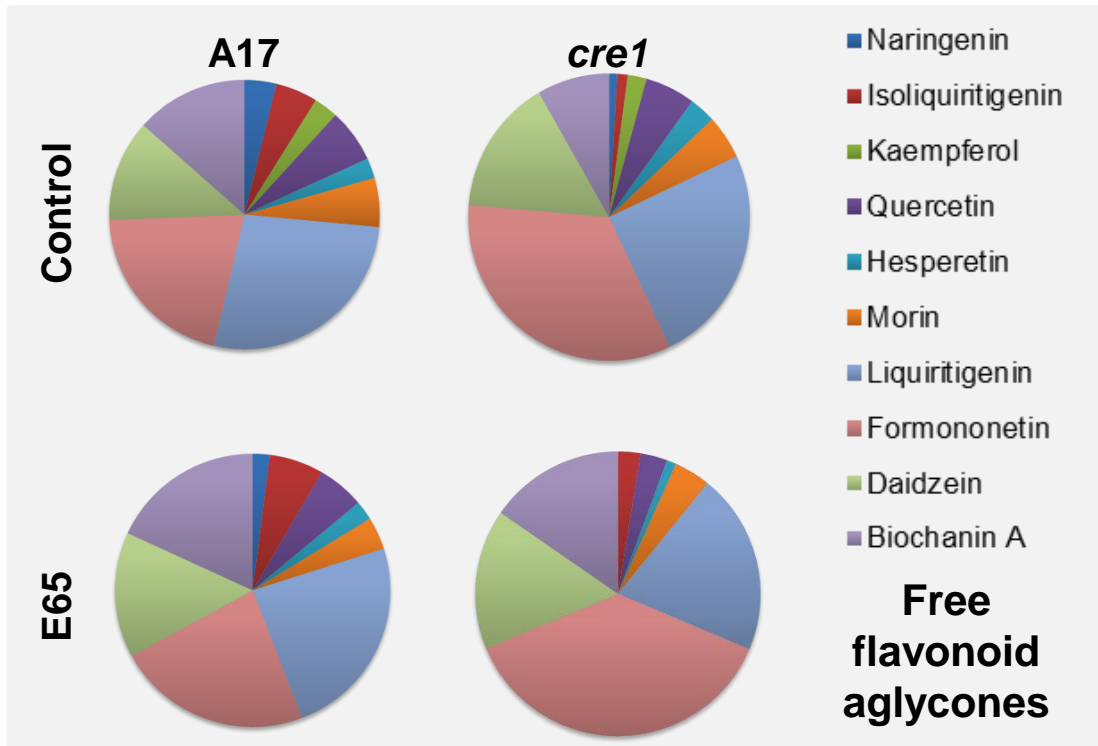


Supplemental Fig. 13. Acropetal auxin transport in roots treated with or without flavonoids, in the presence of E65. Acropetal auxin transport in E65-inoculated roots, with a short-term treatment of kaempferol, quercetin, naringenin or isoliquiritigenin on A17 (A) and *cre1* (B) plants. Acropetal auxin transport in E65-inoculated roots, with a short-term treatment of TIBA or hesperetin in A17 (C) and *cre1* (D). A Tukey-Kramer multiple comparison test was used for statistical comparison between treatments ( $p < 0.05$ ,  $n = 20$ ). Different lowercase letters indicate significant changes in relative auxin transport. Abbreviations: W, water; K, 3  $\mu\text{M}$  kaempferol; Q, 3  $\mu\text{M}$  quercetin; N, 3  $\mu\text{M}$  naringenin; iL, 3  $\mu\text{M}$  isoliquiritigenin; H, 3  $\mu\text{M}$  hesperetin. Graphs show mean and SD.





Supplemental Fig. 14. Basipetal auxin transport in WT and *cre1* mutant roots in response to auxin transport inhibitors at 24 h p.i.. (A) TIBA, (B) flavonoids (A17 only) (3  $\mu$ M) in the absence of rhizobia, (C) quercetin (3  $\mu$ M) in the absence and presence of E65. A two-way ANOVA with a Tukey-Kramer multiple comparison post-test was used for statistical analyses in (A) and (C) ( $p < 0.05$ ,  $n = 20$ ). A Tukey-Kramer multiple comparison test was used for statistical analysis in (B). Different lowercase letters indicate significant changes in relative auxin transport. Abbreviations: W, water; TIBA, 2,3,5-triiodobenzoic acid; K, 3  $\mu$ M kaempferol; Q, 3  $\mu$ M quercetin; H, 3  $\mu$ M hesperetin; iL, 3  $\mu$ M isoliquiritigenin; N, 3  $\mu$ M naringenin. Graphs show mean and SD.



Supplemental Fig. 15. Relative flavonoid abundance (free aglycones) in WT and *cre1* mutant roots in control or E65-inoculated roots. The flavonoids shown here only represent those with absolute quantification data.

Supplemental Table 1 Quality parameters for auxin detection using LC-MS/MS in our study. Commercial auxin standards used in this study and their respective retention times, optimised collision energies, collision induced dissociation high resolution product ions, LODs<sup>a</sup>, LOQs<sup>b</sup>, linearity and correlation coefficients for identification and quantification in positive and negative ion polarity ESI targeted MS/MS.

Analyte	Molecular formulae	MW (g/mol)	Parent Ion [M+H] <sup>+</sup>	Collision energy (eV)	t <sub>R</sub> (min)	Product ions (from most intense to least)					LOD <sup>a</sup> (pg/mg)	LOQ <sup>b</sup> (pg/mg)	Linearity (y = )	Correlation coefficient (R <sup>2</sup> )
						134.0892	133.0826	135.0961	116.9742	95.9716				
<b>D5-IAA</b>	C <sub>10</sub> H <sub>4</sub> D <sub>5</sub> NO <sub>2</sub>	180.21	181.1014	12	12.3 ± 0.004						0.54	0.91	-	-
<b>IAA</b>	C <sub>10</sub> H <sub>9</sub> NO <sub>2</sub>	175.19	176.0710	10	12.4 ± 0.005	130.0643	131.0663	158.0582	103.0522	77.0336	1.01	1.69	20.9120x - 0.1716	0.9991
<b>IBA</b>	C <sub>12</sub> H <sub>13</sub> NO <sub>2</sub>	203.24	204.1033	12	15.7 ± 0.007	186.0890	130.0624	168.0787	158.0934	144.0790	0.20	0.51	34.5990x - 0.3430	0.9976
<b>IAA-Ala</b>	C <sub>13</sub> H <sub>14</sub> N <sub>2</sub> O <sub>3</sub>	246.27	247.1095	10	11.7 ± 0.014	130.0651	90.0553	131.0686	201.1019	-	0.75	1.26	30.9550x - 0.1009	0.9991
Analyte	Molecular formulae	MW (g/mol)	Parent Ion [M-H] <sup>-</sup>	Collision energy (eV)	t <sub>R</sub> (min)	Product ions (from most intense to least)					LOD <sup>a</sup> (pg/mg)	LOQ <sup>b</sup> (pg/mg)	Linearity (y = )	Correlation coefficient (R <sup>2</sup> )
<b>D5-IAA</b>	C <sub>10</sub> H <sub>4</sub> D <sub>5</sub> NO <sub>2</sub>	180.21	179.0874	10	12.2 ± 0.020	135.0960	90.9979	159.6305	59.1363	104.9311				
<b>PAA</b>	C <sub>8</sub> H <sub>8</sub> O <sub>2</sub>	136.05	135.0452	3	11.7 ± 0.047	91.0526	72.0207	117.4564	50.2836	-	6.90	11.50	1.2736x - 0.0050	0.9922
<b>4-Cl-IAA</b>	C <sub>10</sub> H <sub>8</sub> ClNO <sub>2</sub>	209.63	208.0171	8	15.0 ± 0.006	164.0287	165.0275	128.0468	-	-	0.25	0.41	21.5260x + 0.1375	0.9956
<b>IAA-Asp</b>	C <sub>14</sub> H <sub>14</sub> N <sub>2</sub> O <sub>5</sub>	290.28	289.0830	17	9.6 ± 0.059	88.0423	132.0311	115.0051	173.0723	156.0472	1.55	2.58	9.1470x + 0.0279	0.9975
<b>IAA-Ile</b>	C <sub>16</sub> H <sub>20</sub> N <sub>2</sub> O <sub>3</sub>	288.35	287.1361	15	16.5 ± 0.002	130.0854	131.0887	156.0425	243.1475	-	0.05	0.09	97.2150x + 1.1548	0.9959
<b>IAA-Leu</b>	C <sub>16</sub> H <sub>20</sub> N <sub>2</sub> O <sub>3</sub>	288.35	287.1385	10	16.5 ± 0.002	130.0854	131.0887	156.0425	243.1475	-	0.05	0.09	97.2150x + 1.1548	0.9959
<b>IAA-Phe</b>	C <sub>19</sub> H <sub>18</sub> N <sub>2</sub> O <sub>3</sub>	322.37	321.1245	15	16.9 ± 0.007	164.0718	165.0749	147.0453	103.0548	277.1341	0.14	0.24	45.3370x + 0.3456	0.9974
<b>IAA-Trp</b>	C <sub>21</sub> H <sub>19</sub> N <sub>3</sub> O <sub>3</sub>	361.39	360.1354	17	16.4 ± 0.003	203.0829	204.0864	74.0254	116.0514	156.0455	0.76	1.27	6.3667x + 0.1310	0.9914
<b>IAA-Val</b>	C <sub>15</sub> H <sub>18</sub> N <sub>2</sub> O <sub>3</sub>	274.32	273.1243	15	15.1 ± 0.006	116.0739	117.0765	156.0478	128.0522	229.1371	0.11	0.18	58.1590x + 0.3346	0.9987

Injection precision (n=10); data shows mean and SD

<sup>a</sup> Limit of detection (LOD) ≥ 3 x S/N; <sup>b</sup> Limit of quantification (LOQ) ≥ 5 x S/N; S/N, signal-to-noise ratio

Supplemental Table 2 Induction of flavonoid-related genes by the cytokinin BAP, extracted and modified from the publication by Ariel et al. (2012).

16K+ microarray probe ID	Mt genome v4.0-JCVI	Fold Change_BAP vs Control	Adj. P value_BAP vs control	MTG-8 ID and annotation (TIGR database)	Mt genome v4.0-JCVI annotation	Top Uniprot hits
MT000038	Medtr4g031800	2.81	0.00012	TC100176 similar to UPIQ9ZWQ6 (Q9ZWQ6) UDP-glycose:flavonoid glycosyltransferase, partial (83%)	UDP-glucuronosyltransferase ZB5	UDP-glycose:flavonoid glycosyltransferase, Isoflavonoid glycosyltransferase, Terpenoid UDP-glucosyltransferase, Putative UDP-glycose (Fragment),
MT000247	Medtr6g042310	4.24	0.00012	TC100520 weakly similar to UPIQ940V3 (Q940V3) Al2g22590/T9122_3, partial (25%)	Anthocyanidin 3-O-glucosyltransferase	Putative anthocyanidine rhamnosyltransferase, GT4, GT2, UDP-rhamnose:soyasaponin III-rhamnosyltransferase,
MT001043	Medtr6g075830	2.93	0.00102	TC94828 similar to UPIQ8L8C8 (Q8L8C8) Flavanone 3 beta-hydroxylase, complete	Flavanone 3-hydroxylase	Flavanone-3-hydroxylase, Naringenin 2-oxoglutarate 3-dioxygenase
MT001070	Medtr6g033675	4.82	3.00E-05	TC107720 similar to UPIQ9WQ4 (Q9WQ4) UDP-glycose:flavonoid glycosyltransferase (Fragment), partial (66%)	UDP-glucosyltransferase	Flavanone-3-hydroxylase
MT001199	Medtr7g013850	4.32	3.00E-05	TC107840 weakly similar to UPIQ9LRQ7 (Q9LRQ7) Anthocyanin 5-aromatic acyltransferase/benzoyltransferase-like protein, partial (21%)	Anthocyanin 5-aromatic acyltransferase	Anthocyanin 5-aromatic acyltransferase, Isoflavonoid malonyltransferase
MT003127	Medtr2g083390	1.51	0.00379	TC97344	UDP-glucosyltransferase family protein	UDP-glucosyltransferase family protein, Anthocyanidin 3-O-glycosyltransferase, Glycosyltransferase
MT004805	Medtr3g092890	1.85	0.01454	TC96902 similar to UPIQ9FLV0 (Q9FLV0) Flavanone 3-hydroxylase-like protein, partial (82%)	UDP-glucosyltransferase family protein	UDP-glucosyltransferase family protein, Anthocyanidin 3-O-glycosyltransferase, Glycosyltransferase
MT009572	Medtr3g092890	2.65	0.00011	TC109256 similar to UPIQ7XZD0 (Q7XZD0) Isoflavonoid glycosyltransferase, partial (15%)	1-Aminocyclopropane-1-carboxylate oxidase	1-Aminocyclopropane-1-carboxylate oxidase, Oxidoreductase, Flavanone-3-hydroxylase
MT010942	Medtr4g102280	1.90	0.00291	TC111173 weakly similar to UPIQ9ST0 (Q9ST0) Flavonoid 3',5'-hydroxylase-like protein (At4g12310), partial (9%)	Cytochrome P450 family protein	Cytochrome P450, Flavonoid 3'-hydroxylase
MT014304	Medtr2g008220	3.47	0.00012	TC100521 weakly similar to UPIQ940V3 (Q940V3) Al2g22590/T9122_3, partial (15%)	Anthocyanidin 3-O-glycosyltransferase	GT2, GT4, UDP-rhamnose:soyasaponin III-rhamnosyltransferase, Putative UDP-rhamnose:rhamnosyltransferase, UDP-glucosyltransferase,
MT014596	N/A	2.02	0.00112	TC108655 weakly similar to UPIQ7XZD0 (Q7XZD0) Isoflavonoid glycosyltransferase, partial (47%)	UDP-glucosyltransferase family protein	UDP-glucosyltransferase family, GT4, Glycosyltransferase
MT014666	Medtr5g032870	1.55	0.0056	TC102386 weakly similar to UPIQ84UT8 (Q84UT8) Flavonol synthase, partial (25%)	N/A	N/A
MT014842	Medtr6g015320	1.72	0.00474	TC110716 weakly similar to UPIQ9LJB4 (Q9LJB4) Anthocyanin 5-aromatic acyltransferase-like protein, partial (17%)	Malonyl-CoA:isoflavone 7-O-glycoside malonyltransferase	malonyl-CoA:isoflavone 7-O-glycoside malonyltransferase, Putative anthocyanin malonyltransferase, Taxadienol acetyltransferase,
MT014912	Medtr2g046620	3.49	0.00032	TC104594 similar to UPIQ8GVE3 (Q8GVE3) Flavonoid 1,2-rhamnosyltransferase, partial (7%)	UDP-glucosyltransferase family protein	UDP-glucosyltransferase family, Anthocyanidin 3-O-glycosyltransferase, Glucosyltransferase,
MT015597	Medtr2g035020	1.65	0.00017	TC94916 similar to UPIQ7XZD0 (Q7XZD0) Isoflavonoid glycosyltransferase, partial (71%)	UDP-glucosyltransferase family protein	UDP-glucosyltransferase family, Cytokinin-O-glycosyltransferase, Ecdysteroid UDP-glucosyltransferase, Isoflavonoid glucosyltransferase
MT015712	Medtr6g032950	2.03	0.00023	TC109255 similar to UPIQ7XZD0 (Q7XZD0) Isoflavonoid glycosyltransferase, partial (47%)	UDP-glucosyltransferase family protein	UDP-glucosyltransferase family, Cytokinin-O-glycosyltransferase, Ecdysteroid UDP-glucosyltransferase, Isoflavonoid glucosyltransferase
MT015750	Medtr6g032950	2.66	0.00034	TC96991 similar to UPIQ7XZD0 (Q7XZD0) Isoflavonoid glycosyltransferase, partial (51%)	UDP-glucosyltransferase family protein	UDP-glucosyltransferase family, Cytokinin-O-glycosyltransferase, Ecdysteroid UDP-glucosyltransferase, Isoflavonoid glucosyltransferase
MT015828	Medtr2g035040	1.94	0.00493	TC94917 weakly similar to UPIQ7XZD0 (Q7XZD0) Isoflavonoid glycosyltransferase, partial (21%)	Cytokinin-O-glycosyltransferase	GT3, Isoflavonoid glucosyltransferase, Glucosyltransferase, UDP-glycose:flavonoid glycosyltransferase

Supplemental Table 3 Summary table showing the roles of different flavonoid aglycones identified in this study.

Flavonoid	Differential accumulation between WT and <i>cre1</i> roots after rhizobia inoculation	Rescue of nodulation in <i>cre1</i>	Rescue of acropetal auxin transport inhibition in <i>cre1</i>	Rescue of <i>GH3:GUS</i> response in <i>cre1</i> nodule primordia	Expression of genes leading to flavonoid synthesis induced by rhizobia	Expression of genes leading to flavonoid synthesis induced by cytokinin
Naringenin	Yes <sup>1</sup>	Yes	Yes	Yes	Yes	Yes
Isoliquiritigenin	Yes <sup>2</sup>	Yes	Yes	Yes	Yes	Yes
Quercetin	Yes <sup>3</sup>	Partial	Yes	Yes	Yes	Yes
Kaempferol	No	Yes	Yes	Yes	Yes	Yes
Hesperetin	Yes <sup>3</sup>	No	No	No	Yes	Yes
Chrysoeriol	No	Not tested	Not tested	Not tested	No	Yes
Morin	No	Not tested	Not tested	Not tested	Not tested	Not tested
Liquiritigenin	No	Not tested	Not tested	Not tested	Not tested	Not tested
Daidzein	No	Not tested	Not tested	Not tested	Not tested	Not tested
Formononetin	No	Not tested	Not tested	Not tested	Not tested	Not tested
Medicarpin	No	Not tested	Not tested	Not tested	Not tested	Not tested
Biochanin A	No	Not tested	Not tested	Not tested	Not tested	Not tested

<sup>1</sup> Differential accumulation between E65-inoculated WT and *cre1* mutant roots, but no significant induction in WT inoculated vs WT control roots

<sup>2</sup> Differential accumulation in response to E65 inoculation, as well as between inoculated WT and *cre1* mutant roots

<sup>3</sup> Differential accumulation in response to E65 inoculation only in WT but not in *cre1* mutant roots

Supplemental Table 4 Primer sequences of genes used in this study and their gene IDs (v4.0). *PIN5* and *PIN8* mRNAs were not detected in *M. truncatula* roots (Schnabel and Frugoli, 2004).

Gene	Gene ID (Medicago v4.0)	Sequences of primer pairs
<i>PIN1</i>	Medtr4g084870	5'-TGCCCTGAACAAGCTAGGAG-3' ; 5'-GAGACGGGTATAAACACTTGC-3'
<i>PIN2</i>	Medtr4g127100	5'-AGCCTAAGCTGATTGCATGTGG' ; 5'-TGCTATTGAGGTTGCCGCAATC-3'
<i>PIN3</i>	Medtr1g030890	5'-CTTCGCCGGTTCGAAAG-3' ; 5'-GTTTCATCAGCCACCACCACATC-3'
<i>PIN4</i>	Medtr6g069510	5'-GCATGGCTATGTTTCAGTCTTGG-3' ; 5'-GACCAACAAGGAATCTCACACC-3'
<i>PIN6</i>	Medtr1g029190	5'-CAGCCTCGTATCATTGCTTGTG-3' ; 5'-CGGCAATCGAGGATAAGGAC-3'
<i>PIN7</i>	Medtr4g127090	5'-TGTGATTGCGGCAACCTC-3' ; 5'-TGGCAACACAAAAGGGAACG-3'
<i>PIN9</i>	Medtr7g079720	5'-ATGGGTGGATCTTGTG-3' ; 5'-CCCTCTATCCCGTTCTTC-3'
<i>PIN10</i>	Medtr7g089360	5'-TGCCACCTGTAGTATTATG-3' ; 5'-GGGACCAGGTAAGACCAATAAG-3'
<i>LAX1</i>	Medtr5g082220	5'-CTTGGCCTGGCATGACTAC-3' ; 5'-TCTTTGGACCCGAGTGAACC-3'
<i>LAX2</i>	Medtr4g415390	5'-TGGGTTTGGGTTTGGAGGATGG-3' ; 5'-GACTGGTGGTGGTTTGCATTGG-3'
<i>LAX3</i>	Medtr3g072870	5'-GACAGGCTGAGGATGTGAAG-3' ; 5'-AACAGCATGTCCACCAAAAGG-3'
<i>LAX4</i>	Medtr4g415390	5'-TGGAGGATGGGCTAGTATGACC-3' ; 5'-ATGGTCTTGAGGTGGTGTGG-3'
<i>LAX5</i>	Medtr4g073770	5'-CCACCGTTGGATCTACTTG-3' ; 5'-CATTCTGTCGAGCAGAGGGATG-3'
<i>GH3</i>	Medtr5g016320	5'-CTCAGAGTTTCTGACCAGTTCAG-3' ; 5'-AGTAGGCTGTACAATAACTGACGAC-3'
<i>CHS</i>	Medtr7g016780	5'-CACCTTCGTGAAGCTGGACT-3' ; 5'-GTGGCTCAAAAGCGTCAACC-3'
<i>CHR</i>	Medtr5g097900	5'-TTGGCCACTTAGCTCTCAGC-3' ; 5'-CCATGGATTCCCAACACCCC-3'
<i>CHI</i>	Medtr1g115870	5'-CCACGAGCTCCTATCCT-3' ; 5'-ACTGCTGTCTCAACCTCTGG-3'
<i>F3H</i>	Medtr3g025230	5'-CACCTTATGGTCCGGGTG-3' ; 5'-TACCTCTTCTGACGCAAGT-3'
<i>FLS</i>	Medtr5g032870	5'-GTGACCAACAATGTGCAACC-3' ; 5'-TTGGAGGGTGTCTTTCATC-3'
<i>FLS</i>	Medtr4g100590	5'-GGTGCCTCTGCTCATTGATTCAG-3' ; 5'-CCACACCTGAGGTTGCTTCA-3'
<i>GAPdh</i>	Medtr3g085850	5'-TGCCTACCCTGATGTTTTCAGT-3' ; 5'-TTGCCCTCTGATTCCTCCTTG-3'
<i>RBP1</i>	Medtr6g034835	5'-AGGGCAAGTTCTTCATTT-3' ; 5'-GGTAGAAGTCTGGCTCAGG-3'